Journal of Applied Polymer Science

Mechanical and Barrier Properties of Thermoplastic Whey Protein Isolate/Ethylene Vinyl Acetate Blends

Markus Schmid,[1,2*] Kerstin Müller,[1,3*] Sven Sängerlaub,[1,2] Andreas Stäbler,[1] Vanessa Starck,[1] Felix Ecker,[3] Klaus Noller[1]

[1]Fraunhofer Institute for Process Engineering and Packaging IVV, Giggenhauser Strasse 35, Freising 85354, Germany

[2]Chair for Food Packaging Technology, Technische Universität München, Weihenstephaner Steig 22, Freising 85354, Germany

*These authors contributed equally to this work.

[3]Department of Food Technology, Hochschule Fulda—University of Applied Sciences, Marquardstraße 35, Fulda 36039, Germany

Correspondence to: M. Schmid (E-mail: markus.schmid@ivv.fraunhofer.de)

ABSTRACT: Crude oil is becoming scarcer and more expensive, resulting in alternative biobased or partially biobased materials gaining importance in the field of plastic packaging and encouraging the development of naturally derived, protein-based plastics (Endres, 2009; Jones and McClements, *Compreh. Rev. Food Sci. Food Safety* 2010, 9, 374; Khwaldia et al., *Compreh. Rev. Food Sci. Food Safety* 2010, 9, 374). A strategy to improve extrusion processing behavior of proteins is the blending with other polymers. In this study ethylene vinyl acetate (EVA) was used for such purpose. The aim of this study was to determine the properties of blends of thermoplastic whey protein (TPP) and ethylene vinyl acetate (EVA). Mechanical and barrier properties were tested. Blends of differing TPP/EVA ratio were produced and extruded into flat films. Morphological analysis of the blends shows immiscibility of the TPP and EVA, greatly influencing the mechanical properties. Young's modulus measurements shows the values approached that of pure EVA with increasing EVA ratios. At values of about 21 MPa, corresponding to EVA ratios of 30% (w/w) and above, continuous extrusion including material take-off was possible. At higher whey protein ratios in the blends the water vapor transmission rate increased, i.e., the higher water vapor transmission rate of whey protein compared with EVA dominated this property. This study showed that whey proteins can be utilized for extrusion by blending with EVA. © 2014 Wiley Periodicals, Inc. J. Appl. Polym. Sci. **2014**, *131*, 41172.

KEYWORDS: blends; extrusion; films; functionalization of polymers; mechanical properties

Received 14 April 2014; accepted 12 June 2014

DOI: 10.1002/app.41172

INTRODUCTION

Because of the high amount of plastic trash and the scarcity and rising cost of fossil fuels, the development of biodegradable and/or bio-based polymers is gaining importance. Biopolymers based on renewable resources such as starch, cellulose and proteins are considered promising for the processing to packaging materials. The differing molecular structure of proteins causes different properties of films made thereof such as specific barrier and mechanical properties.[1–3] This means that packaging materials can be produced with a wide range of functional properties.[4] For this reason, protein-based materials might be suitable for replacing or complementing the hitherto used fossil fuel-based polymers in food packaging applications.

Whey is one of the biggest sources of food protein, but only a small fraction of this is consumed by humans.[5] Approximately 92% of the produced whey is an unused by-product of cheese production.[6] There is a growing demand to find ways of using that whey. Up until now several processes for forming whey protein based films and coatings and their properties have been studied. The barrier properties were one focus of these studies.[7–13] Recent studies showed that whey protein based layers generated by lacquering processes have excellent barrier properties with oxygen permeability (OP) $Q_{100} < 1.5$ cm^3 (STP) m^{-2} d^{-1} bar^{-1} and water vapor transmission rate (WVTR) $Q_{100} < (2-3)$ g m^{-2} d^{-1} 85→0 % relative humidity, 23°C,[14–20] making them suitable for use in sensitive food packaging applications.[21]

Extrusion is another continuous processing technique of practical industrial use for whey protein based films or separate layers in multilayer films. However, the materials here must have thermoplastic properties. As proteins have no natural thermoplastic behavior, the use of additives is indispensable for extruding proteins.[22] Proteins can undergo a large number of interactions due to the different functional groups in the amino acid side chains. These allow a vast number of interactions and chemical

reactions to take place during thermal processing, such as denaturing and crosslinking.[23] These reactions can be modified or influenced by additives to alter the polymer conformation. The addition of plasticizers to whey protein-based formulations enables thermoplastic processing and hence film extrusion. Hernandez et al. developed appropriate formulations for such processes using a mixture of glycerol and water (70 : 30) for whey protein isolate (WPI) plasticization in an extrusion process.[24] During extrusion, covalent crosslinks (disulphide bonds) are formed inhibiting the formation of a thermoplastic material. Reducing agents for disulphide bridges such as sulphite can be used to prevent extensive crosslinking, enhancing protein chain mobility and giving lower apparent viscosities during extrusion processing.[25] Unfortunately, the mechanical properties and continuous processability of up to now produced thermoplastic protein (TPP) films are still limited.

Other bio-based plastics such as starch based plastics have the same problems. Here, a common technique to overcome these limitations is the production of starch–polymer blends.[26] Gupta and Nayak[27] examined blends of different proteins with natural and synthetic polymers and noted the improved properties of whey protein/cellulose blends and soy protein/agar blends. Likewise, blends of TPP with Ethyl-Vinyl-Acetate (EVA) could potentially offer enhanced mechanical properties and enable a continuous extrusion process. EVA was chosen due to the wide processing window and suitable processing temperature (30–110°C) in combination with TPP at which thermo-degradation can be avoided or reduced. In other studies EVA was blended with different polymers such as high-density polyethylene (PE-HD), low-density polyethylene (PE-LD), ground tyre rubber, polypropylene (PP), poly(ethyleneterephthalate) (PET), and polyamide 6 (PA6) as well as with nanoclays which indicates that EVA is well suitable for blending with other polymers and particles.[28–35]

Previous studies have, however, already demonstrated the suitability of whey protein formulations for packaging materials. Consequently, the objective of this study was to investigate the technofunctional properties of up to now not studied thermoplastic whey protein containing blends for food packaging based on TPP and EVA. In particular, it was investigated how the barrier, mechanical, morphological and optical properties change on varying the concentration of EVA. Furthermore, a blend ratio suitable for continuous flat-film extrusion was identified. The ever growing demands for alternative packaging materials fully or partially based on renewable resources or currently underutilized raw materials means that this work has economic and industrial relevance and makes a contribution to future applications of thermoplastic whey protein-based packaging materials.

EXPERIMENTAL

Materials

Whey protein isolate BiPro and hydrolyzed whey protein isolate (h-WPI) BioZate 3 (degree of hydrolysis 10%) were purchased from Davisco Foods Intl. Inc. (Le Sueur, MN). Sodium sulphite was obtained from Sigma Aldrich Chemie GmbH (Steinheim, Germany); glycerol was supplied by Merck KGaA (Darmstadt, Germany). Deionized water was supplied by the Fraunhofer IVV in Freising, Germany. The EVA Evateno HM 150 was purchased from Braskem Europe GmbH (Frankfurt am Main, Germany) and had a vinyl acetate content of 20% (w/w).[36] The melting point is 83°C.

Compounding

The thermoplastic protein formulation (TPP) was compounded using a Haake Rheocord with Rheomex PTW 16 corotating twin screw extruder (Thermo Fisher Scientific, Karlsruhe, Germany) with a length to diameter ratio of 25. The general formulation of the TPP material was WPI (90 parts), h-WPI (10 parts), sodium sulphite (5 parts) and a glycerol/water mixture (70 : 30 (w/w); 100 parts). Solid feed (WPI, h-WPI, sodium sulphite) with a feed rate of 0.8 kg h^{-1} was performed with a gravimetric twin-screw loss-in-weight feeder placed on a scale platform (K-Tron AG, Niederlenz, Switzerland) and took place in the first zone of the barrel. Liquid feed was performed with an Ecom Alpha 50 Plus isocratic pump (Ecom spol. s r.o., Prague, Czech Republic) and took place in the second zone of the barrel. The screw speed was 200 rpm with a barrel temperature profile of 0–40–80–110–130 (°C). The extrudate was pelletized using a CSG 171 T strand pelletizer (Dr. Collin GmbH, Ebersberg, Germany). Blends with EVA were compounded in ratios of 100/0, 50/50, 40/60, 30/70, 20/80, 10/90, and 0/100 EVA/TPP at 200 rpm using a corotating twin screw extruder ZK 27 T × 24 D (Dr. Collin GmbH, Ebersberg, Germany) with length to diameter ratio of 24 and pelletized directly after extrusion. Barrel temperatures in zone 1–5 were constant at 17–20–50–70–75 (°C) and the die temperatures varied depending on the formulation from 100°C to 130°C.

Flat Film Extrusion

Sheets were extruded from pellets prepared as described above using a single screw extruder E-20P (Dr. Collin GmbH, Ebersberg, Germany) with an *L/D* ratio of 25. The extruder was followed by a cooling/heating chill-roll/calendar-item with an edge trim and a winder. The highest barrel temperatures varied from 100°C to 150°C, and die temperatures were 110°C to 140°C depending on the formulation. The screw speed was 180 rpm. Sheets were drawn with a take-off speed of 0.4 m min^{-1} (samples with 30% EVA and above) at the take-off unit. The thickness of the extruded films ranged from ~0.8 mm to 1.8 mm.

Color Determination

The CIE-$L^*a^*b^*$ color space is divided by three orthogonal coordinate axes L^*, a^*, and b^*. L^* values define the lightness of a color, where $L^* = 0$ indicates black and $L^* = 100$ indicates white. The parameter a^* displays the red–green axis, where negative values are green and positive values are red. The b^* axis defines yellow and blue color, where negative values are blue and positive values are yellow.[37] A CM 700 d spectrometer of Konica Minolta (Sensing, Germany) with SAV aperture (Φ3 mm/Φ6 mm) was used to measure the color of the samples. Before the measurements, zero and white calibration were performed according to the Konica Minolta calibration procedure. For each specimen a five-fold determination was performed. Color values are given within the CIE-$L^*a^*b^*$ color space. Only color values without gloss (SCE) were considered.

Thickness Measurements

Thickness measurements for mechanical and barrier tests were performed with a precision thickness gauge FT3 (Rhopoint

Instruments, Beyhill on Sea, UK) at five random positions around the film testing area and averaged for the thickness determination.

Mechanical Properties

Before the sheets were cut into strips of 15 × 150 mm^2 they were stored at 23°C and 50% RH for at least one week to reach equilibrium. The elongation at break, tensile strength and Young's modulus were measured using a tensile testing machine Z005 (Allround Line) of Zwick GmbH & Co. KG (Ulm, Germany) following the DIN EN ISO 527-1 method. Tests were performed in the machine direction with a clamping length of 50 mm. The test speed was 200 mm min^{-1} with a load shut-off at 95%. Five replicates were tested for each sample.

Calorimetric Analysis

The specimens were stored at 23°C and 50% RH for at least 1 week before sample preparation. Differential scanning calorimetry (DSC) was performed on a DSC 821e instrument of Mettler-Toledo GmbH (Gießen, Germany) following the DIN EN ISO 11357-1 method. Specimens were heated from −50°C to 200°C at a heating rate of 10 K min^{-1}. Two heating runs were performed with approximately (10–30) mg of sample.

Morphology Analysis

For morphology analysis, microtome sections of 20 μm thickness were prepared with an Autocut 2055 of Leica Microsystems GmbH (Wetzlar, Germany). The phase composition was examined in transmission mode using a Leica Microsystems Dioplan optical microscope at 40× and 200× magnification.

Permeation Measurements

Water Vapor Transmission Rate (WVTR). The water vapor transmission rate was measured following the DIN 53122-1 method. The initial sample weight was determined with an analytical balance Mettler H315 of Mettler-Toledo GmbH (Gießen, Germany) and the cups were filled with dried silica gel then stored in a climate chamber manufactured by Binder GmbH (Tuttlingen-Möhringen, Germany) at 23°C and 85% RH. The samples were weighed four times in 48 h until the weight gain was constant. Four replicates were tested for each sample. To compare water vapor transmission rates of different films, *WVTR* Q_{100} values were calculated as follows:

$$WVTR\,Q_{100} = WVTR * \frac{d}{100\,\mu m} \quad (1)$$

WVTR: measured water vapor transmission rate [g m^{-2} d^{-1}, 85→0% RH] d: film thickness [μm]

Oxygen Permeability (OP). The oxygen permeability was measured using the oxygen-specific carrier gas method according to DIN 53380-3. Measurements were performed with an Ox-Tran Twin Oxygen Permeation Measuring Machine (Mocon, Minneapolis, USA). Measurements were carried out at a temperature of 23°C and 50% RH. For each sample two-fold determination was performed. To compare the oxygen permeability of different films, *OP* Q_{100} values were calculated as follows:

$$OP\,Q_{100} = OP * \frac{d}{100\,\mu m} \quad (2)$$

OP: measured oxygen permeability [cm^3(STP) $m^{-2}d^{-1}$ bar^{-1}] d: film thickness [μm]

Statistical Methods

The experimental design for statistical evaluation was performed by the computer program Visual-XSel 12.0 Multivar (CRGRAPH, Munich, Germany). All measured data were tested for normal distribution. Depending on the sample size, either the Kolmogorov-Smirnov test (in the case of a sample size of four) or Anderson-Darling normality test (in the case of sample sizes of five or more) were used with a significance value α of 0.05. The mean values of OP were calculated from two-fold determinations. These data were not tested for normal distribution, therefore minimum and maximum values are given for evaluation. The Hampel test for outliers was used to detect outliers at a significance value α of 0.05. The condition for elimination was that all other values are part of the same population, as proved by normality tests described above. For sample set comparison, a multi-*t*-test was applied using a significance value of 0.05.

RESULTS AND DISCUSSION

Compounding

To enable thermoplastic processing of proteins without material degradation, whey protein isolate was plasticized with a glycerol/water mixture. To prevent extensive crosslinking, leading to a thermoset material, sodium sulphite was used as a masking agent for chemical modification. Both additives were essential for successful compounding. Previous studies showed that WPI replacement by h-WPI had a positive influence on film flexibility as indicated by the decrease in the Young's modulus of solution cast WPI films.[17] Therefore, h-WPI was used in the TPP formulation. Thermoplastic protein extrusion has strict limitations with regard to the temperature processing window. Based on pretrials it was observed that above ∼150°C protein degradation starts and extrusion processing is not possible. Using the selected process parameters, pure TPP as well as blends containing up to 50% (w/w) EVA were produced in a continuous process with acceptable melt pressures.

Flat Film Extrusion

Pure TPP, TPP/EVA blends with EVA contents up to 50% (w/w) and pure EVA were extruded as flat films. Rewinding of pure thermoplastic protein formulations was not possible. With increasing EVA content, melt stability within the process increased, enabling continuous thermoplastic process. At ratios of 30% (w/w) EVA and above, material take off was possible without tearing of the film.

Color Determination

Extrusion of pure EVA produces transparent films. Blending it with TPP led to a yellowish color (Figure 1). For the following characterizations, blends with an EVA content of up to 50% (w/w) as well as pure TPP and pure EVA were used. The b^* value provides the most useful information since it corresponds to the yellow ($b+$) and blue ($b-$) axis in the CIE-$L^*a^*b^*$ color

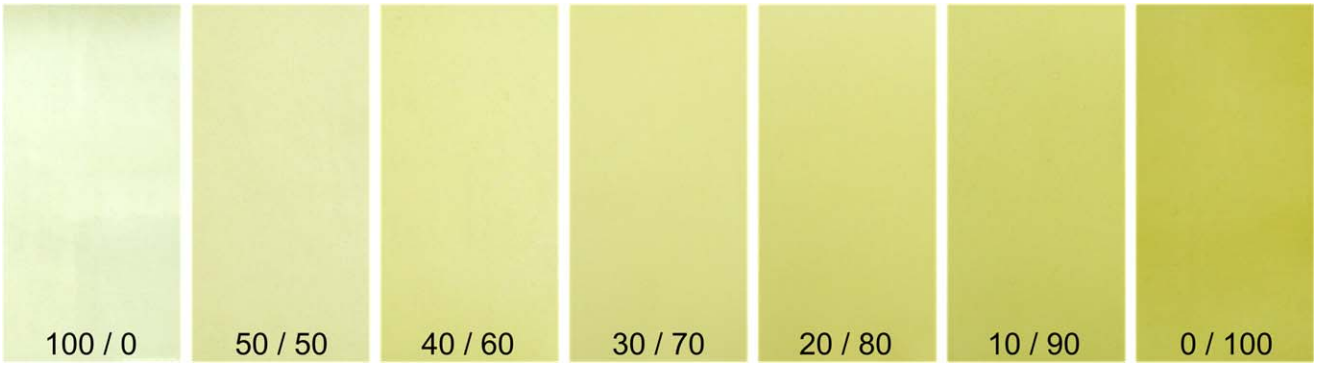

Figure 1. EVA/TPP films with different blend ratios (EVA [%] / TPP [%]). [Color figure can be viewed in the online issue, which is available at wileyonlinelibrary.com.]

space. The more positive the b^* value, the more yellow the sample.[37] Figure 2 shows the respective b^* values of the samples.

Pure EVA, which is transparent to the human eye, has a b^* value of 3.20 and therefore has a slightly yellowish color. With rising TPP content, the values increased approximately linearly starting from the 50 : 50 ratio. Significant differences were found at every concentration step performed. Hernandez et al. who extruded glycerol/water (70 : 30; (w/w)) plasticized WPI films also observed a yellowish discoloration.[23] This can be explained by the yellow metabolites in WPI and h-WPI, with h-WPI assumed to contain a larger number of yellow whey metabolites than nonhydrolyzed WPI.[21] Generally the measurements showed that with rising protein concentration the b^* color values of the whey protein-based films also rose due to the yellowish metabolites.

Mechanical Properties

Young's Modulus. Figure 3 shows how different EVA ratios influence the Young's modulus. The measured Young's modulus of pure EVA with circa 28 MPa was higher than at an EVA with 28% (w/w) and 27% (w/w) of vinylacetate with circa 16 MPa[35] and circa 12 MPa[38] and lower than that found at an EVA with 18% (w/w) vinyl acetate content with circa 75 MPa.[32] Young's modulus increases from the material with the lower value (TPP) to the material with the higher value (EVA) which harmonizes the results of groups for polymer blends, such as LDPE/EVA-blends[32] and PVC/PU-blends.[39] However, for 20% (w/w) EVA addition and above, differences were statistically not significant ($P > 0.05$). As Young's modulus is determined at very low elongations, the disruption of the continuous protein phase by the added EVA only has a minor impact on the measured values compared to other mechanical properties such as elongation at break and tensile strength. At values of about 21 MPa and higher, material rewinding was possible enabling a continuous extrusion process with adapted chill roll parameters.

Tensile Strength. Figure 4 shows tensile strength values of TPP/EVA, pure TPP, and pure EVA films. The tensile strength pure EVA with circa 8 MPA was similar to EVA with 28% (w/w) of vinylacetate with circa 9 MPA[35] but lower than EVA with 18% (w/w) and 27% (w/w) of vinylacetate with circa 21 MPa[32] and circa 28 MPa.[38]

Compared with the TPP material and tested TPP/EVA-blends, the tensile strength of the EVA is more than four times higher. Blending with EVA reduces the tensile strength of TPP significantly ($P \leq 0.05$). However, at a concentration from 20 to 50% (w/w) EVA the tensile strength slightly increases but is more than factor four below EVA. The observed behavior is opposite to PE-LD/EVA-blends[32] at which the tensile strength steadily increases with EVA concentration. However, PVC/PU-blends showed similar behavior such as TPP/EVA-blends was found.[39] The tensile strength of PU reduced at an increasing PVC

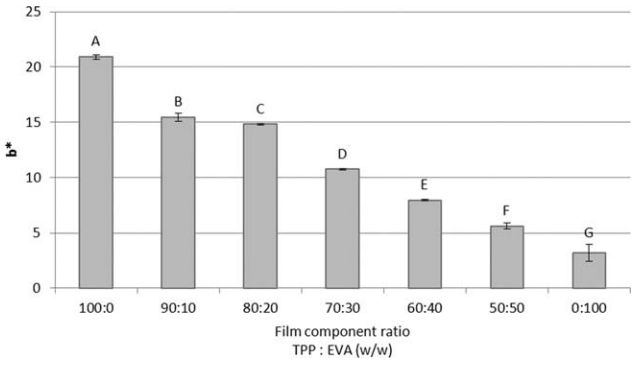

Figure 2. Influence of the EVA ratio on the b^* color value (SCE) of EVA/TPP blends. Columns with different letters are significantly different ($P \leq 0.05$).

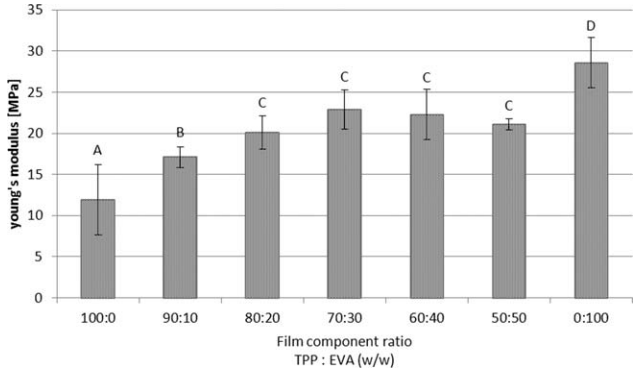

Figure 3. Young's modulus of TPP/EVA films as a function of the EVA concentration. Columns with different letters are significantly different ($P \leq 0.05$).

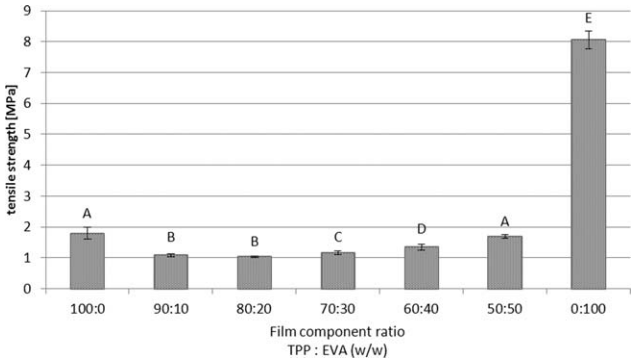

Figure 4. Tensile strength of TPP/EVA films as a function of the EVA concentration. Columns with different letters are significantly different ($P \leq 0.05$).

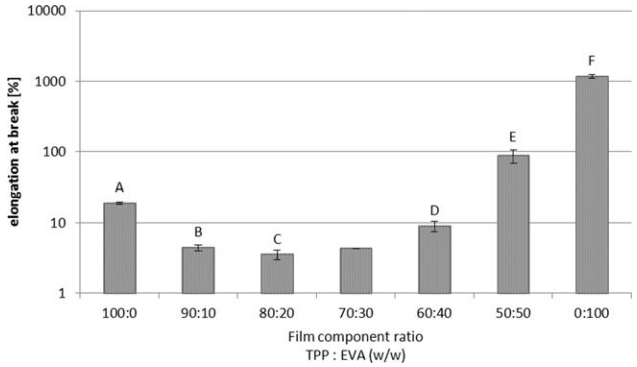

Figure 5. Elongation at break of TPP/EVA films as a function of the EVA concentration. Columns with different letters are significantly different ($P \leq 0.05$).

content with the lowest tensile strength at a ratio of 50 : 50 (w/w) and increased at a higher PVC content.

The behavior can be explained by disrupting of the protein network at higher EVA content until the EVA forms a continuous phase and its tensile properties dominate.

Elongation at Break. The elongation at break with circa 1170% was lower than the strain of break of EVA with 27% (w/w) of vinylacetate with circa 1400%[38] and higher than EVA with 18% (w/w) vinylacetate with circa 900%.[32] Blending of TPP with EVA reduces the tensile strength. At an EVA content of 40% (w/w) the elongation at break increased. This parabolic shape of the elongation at break as function of the EVA-content was not observed at PE-LD/EVA-blends[32] and PVC/PU-blends[39] which showed at steady increase from a lower to a higher value. Just as for the tensile strength values, the addition of EVA in lower ratios disturbed the protein network. The resulting weak points or flaws in the network caused a significantly lower ($P \leq 0.05$) elongation at break (see Figure 5). Compared with pure TPP films, the elongation at break only increased at an EVA concentration of 50% (w/w). The significant increase ($P \leq 0.05$), by more than four times the pure TPP values, may indicate a change in the morphology of the two phases present. The larger the coherent amounts of the EVA phase, the closer the properties of the pure material are approached.

At 30% EVA concentration, the measured values were the same at the given measurement accuracy and therefore neither the standard deviation nor multi-*t*-test could be determined.

Even though the mechanical properties of the blends are quite less good compared with pure EVA and other standard polymers, their application in combination with paper and board could be sufficient for packaging applications.

Calorimetric Analysis

Differential scanning calorimetry can be used to characterize thermal transitions in polymers. With regard to proteins and protein-plasticizer thermal transitions, DSC can be used to detect events such as the glass transition temperature (T_g), melting, thermal denaturation, aggregation, and protein degradation.[23] To determine the glass transition temperature, melting range, denaturation, and degradation temperatures, the TPP and blended films were analyzed via DSC. Although the main caloric effects in TPP films were mainly interfered with by the evaporation of residual water, an endothermic peak was determined at a temperature of 146.5°C. As a second heating run showed no transitions in this temperature range, the peak can be assigned to irreversible denaturation. Hernandez et al. who extruded glycerol/water plasticized WPI films also measured a denaturation temperature of (148.3 ± 0.7)°C.[23] After the denaturation of the residual native protein, material degradation starts at ~180°C. The glass transition temperature of dry proteins (less than 5% water) lies close to or even above their decomposition temperatures.[40] In general, a plasticizer lowers the T_g of biopolymer films. This means the rubbery state is extended to a broader temperature range, giving improved flexibility and stretchability of the films.[41] Plasticization is essential for the thermoplastic extrusion processing of proteins. The use of glycerol/water mixtures in the TPP formulation lowered the T_g to −19.6°C, showing the plasticizing effect of glycerol and water. Anker et al. measured similar glass transition temperatures of −17°C (pH 7) for sorbitol plasticized WPI cast films.[42] Zhang et al. also used DSC to determine the T_g of extruded soy protein sheets plasticized with 30 parts of glycerol and different ratios of water. The glass transition temperatures of the sheets ranged between −7°C and 50°C depending on the water content.[43] The lower T_g of TPP extruded sheets can probably be ascribed to the higher glycerol content. Sothornvit et al. studied the glass transition temperatures of glycerol plasticized (0.21*M*) β-lactoglobulin cast films, measuring a T_g of (-45.09 ± 2.63)°C.[41] However, when comparing biopolymer T_g values interference from other thermal events such as crystallization and enthalpic relaxation that obscure the determination as well as the history of thermal treatment must be considered.[41,44] Pure EVA showed a glass transition temperature of −17.22°C and a melting point of 82.44°C. When TPP was blended with EVA, DSC showed that the EVA melting point was at a constant temperature and that the protein denaturation temperature varied depending on the blend ratio. Generally, the addition of EVA lowered the denaturation temperature of TPP in all blended ratios. In immiscible materials each specific T_g can usually be determined. When glass transition temperatures were observed in TPP/EVA blends only one glass transition point could be determined. This could be due to the similar T_g temperatures of about −20°C for the materials in the blends.

Table I. Protein Denaturation and Glass Transition Temperatures of TPP/EVA Blends

Film component ratio TPP : EVA (%)	T_g (°C)	Denaturation[a] (°C)
100 : 0	−19.55	146.45
90 : 10	−21.49	139.79
80 : 20	-	143.71
70 : 30	−16.06	139.71
60 : 40	-	131.76
50 : 50	−17.52	136.29

[a] Irreversible denaturation peak.

The measured denaturation and glass transition temperatures are shown in Table I.

Morphology Analysis

To determine the morphology and in particular the phase distribution of the blends, microtome sections were prepared. Images of all blends as well as pure EVA and TPP films are shown in Figure 6.

Two phases were observed for all blend ratios. As seen for the pure material, EVA is the blue colored phase while the protein part is grey/black. The structure indicated immiscibility of TPP and EVA. Other research groups found similar structures in PA/EVA-blends,[30] HDPE/EVA-blends,[32] Nylon 6/ethylene propylene rubber (EPM)-blends,[45] and PP/EVA-blends.[29]

At EVA contents up to 30% (w/w), the EVA spheres are dispersed in the continuous TPP domain. At these concentrations the EVA spheres start to form a continued network. Interestingly at starch/polyethylene blends a similar behavior was observed. At a starch content higher than circa 30% (w/w) it the starch particles connected.[46] At stretched calcium carbonate/PE films an overproportional increase of connectivity was found as well at more than 40% (w/w) calciumcarbonate content which resulted in an highly in increasing water vapor transmission rate.[47]

When the tested materials are under stress, the continuous phase, here TPP, absorbs most of the stress and energy. Because

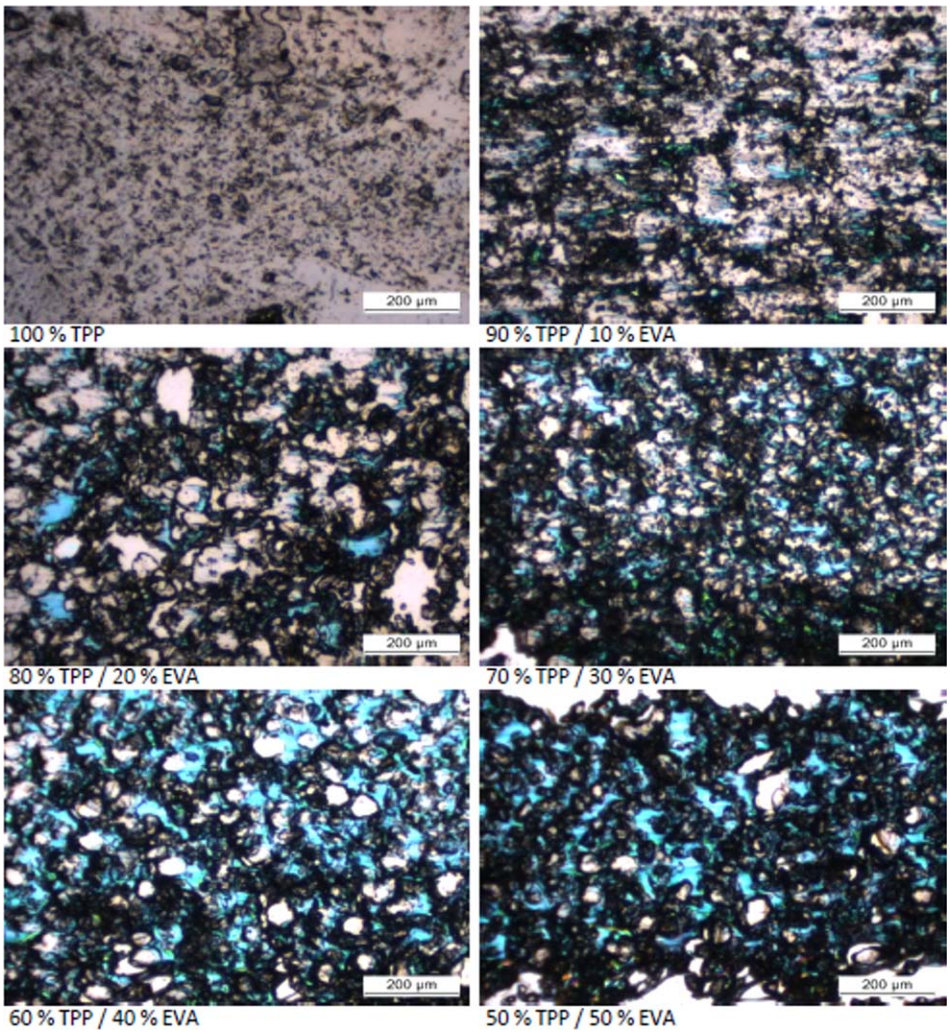

Figure 6. Microtome sections of TPP/EVA blends and pure TPP observed under an optical microscope. Images were taken at ×40 magnification. [Color figure can be viewed in the online issue, which is available at wileyonlinelibrary.com.]

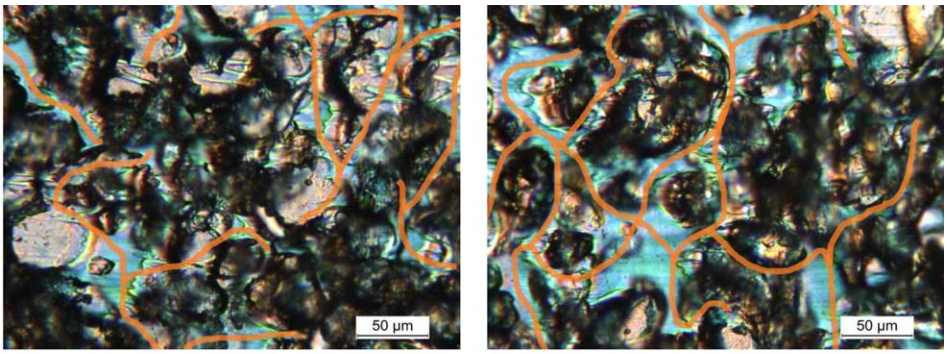

Figure 7. Microtome sections of selected TPP/EVA films under an optical microscope at ×200 magnification. Continuous EVA domains are outlined in orange. [Color figure can be viewed in the online issue, which is available at wileyonlinelibrary.com.]

of this, the mechanical properties are like those of the pure TPP material, although the blends are weaker than a sample of pure TPP. This is also consistent with the mechanical properties described earlier. With increasing EVA content there was contraction or maybe even agglomeration of the proteins within the TPP matrix. These agglomerates fall out when sectioning the films, causing holes within the cut sections (white color). The occurrence of two separate polymer domains indicates immiscibility of the materials. However, when concentration of EVA and TPP are almost equal or actually equal, both phases seem to exist co-continuously. Blends with a co-continuous phase distribution have tightly intermeshed structures facilitating load transfer across interfacial areas and thus optimizing the mechanical properties.[48]

Co-continuous structures can normally form around the phase inversion composition. However, such structures also occur independently of phase concentrations during phase inversion processes in blends in which the component finally displaying the dispersed phase forms the matrix in early mixing states.[49] For a better understanding of the morphology and the phase dispersions at these concentrations, Figure 7 shows the microtome sections at higher magnification.

On comparing EVA concentrations of 40% and 50% (w/w), an enlargement of the coherent EVA phase is evident for the 50% (w/w) concentration. Here, the change from a disperse phase distribution to co-continuous phase can be observed. When such a material is under stress, both polymers absorb the energy. Thus the mechanical properties can no longer be described by referring to just one of the polymers but must be described by the coexisting domains.[49] This effect is also consistent with the change in the mechanical properties at these EVA concentrations.

Permeation Measurements

Water Vapor Transmission Rate (WVTR) at (85→0)% RH. Pure TPP showed a water vapor transmission rate normalized to 100 μm film thickness [see eq. (1)] of ~18,000 g m^{-2} d^{-1}. Other literature cites WVTR Q_{100} values of 33,600 g m^{-2} d^{-1} for compression moulded WPI/glycerol films (1 : 1).[50] However, solution casting with higher protein contents (WPI:glycerol 1.6 : 1) gave WVTR Q_{100} values of 12,000 g m^{-2} d^{-1}. This difference could also be related to the protein structure, since higher molding temperatures cause greater crosslinking and therefore less soluble proteins within the network.[23] Extruded TPP films seem to lie in between the two film formation processes mentioned above with regard to their water vapor barrier properties. Generally, the low water vapor barrier of the samples can be assigned to the highly hydrophilic plasticizer enabling diffusion within the film material. However, when TPP was blended with EVA in different ratios the WVTR values decreased significantly ($P \leq 0.05$) for each step (see Figure 8).

However, the WTVR values for 30% EVA were almost halved with further EVA addition and did not decrease as sharply as before. Morphology analysis showed there was a co-continuous phase distribution in these blends (40% and 50% EVA), leading to fewer contact interfaces than in the disperse phase distribution. At an EVA concentration of 50% (w/w), the WVTR Q_{100} values decreased by a factor of greater than 10 compared with

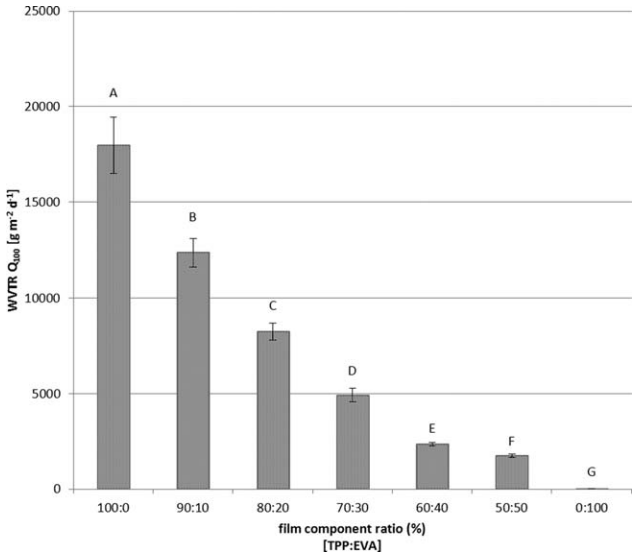

Figure 8. Water vapor transmission rates for TPP/EVA films normalized to 100 µm thickness. Columns with different letters are significantly different ($P \leq 0.05$).

the pure TPP material. Thus blending with EVA greatly enhanced the water vapor barrier properties of TPP.

Oxygen Permeability (OP). For all measured samples the oxygen permeability values showed wide variation and were sometimes not even evaluable. However, the lowest measured values indicate potential barrier properties. The pure TPP formulation showed the lowest oxygen permeability of 3.75 cm^3(STP) m^{-2} d^{-1} bar^{-1} and an OP Q_{100} value of 52.3 cm^3(STP) m^{-2} d^{-1} bar^{-1}. As pure EVA does not have good oxygen barrier properties [OP Q_{100} 5204.5 cm^3(STP) m^{-2} d^{-1} bar^{-1}], blending with TPP was expected to enhance the barrier properties with increasing TPP ratio. With 50% (w/w) TPP addition, the OP Q_{100} value was found to decrease by more than 93%. The assumption that increasing TPP values would also increase oxygen permeability was not supported by the measurement series performed, because samples with TPP contents of 60 and 70% gave higher values than the blends containing 50% TPP. All were single determinations and so measurement uncertainties must also be considered here.

CONCLUSIONS

With sodium sulphite modification and plasticization with glycerol and water, the thermoplastic processing of whey proteins into films was generally found to be possible. The mechanical properties of TPP could not withstand a continuous extrusion process, meaning that material rewinding via chill-roll was not feasible. However, a continuous thermoplastic process for flat film extrusion using suitable polymer–protein blends was possible. The EVA polymer that was used improved the mechanical properties as well as the process stability. Young's modulus measurements showed that with increasing EVA ratio the values approached that of pure EVA. At values of about 21 MPa, corresponding to EVA ratios of 30% (w/w) and above, material take-off at low rewinding speed was possible without web-tearing.

Morphological analysis of the materials showed immiscibility of the two blended components. However, at ratios of 40 and 50% (w/w) EVA there were continuous domains that significantly influenced the mechanical properties and processability.

Pure TPP sheets showed high water vapor transmission rates (WVTR $Q_{100} \sim 18{,}000$ g m^{-2} d^{-1}). However, when TPP was blended with EVA in different ratios, the WVTR values decreased. At an EVA concentration of 50% (w/w) the WVTR Q_{100} values decreased by greater than a factor of 10 compared with the pure TPP formulation. Based on this, it can be concluded that the blending of whey protein based formulations with EVA can be used to enhance the water vapor barrier properties of TPP films.

Although the oxygen barrier measurements could not be statistically evaluated, the lowest measured values confirm certain barrier properties. The use of TPP as a blend partner with other low oxygen barrier thermoplastic materials could therefore be considered for adapting the oxygen permeability of such blends.

Other research groups found that the melt mixing temperature, mixing time, and annealing time influences the blend morphology.[32,45] The influence of these parameters should be tested in further studies. Furthermore, the influence of additives such as nucleating agents and antioxidants on the morphology and stability should be analyzed.[22]

ACKNOWLEDGMENTS

The authors wish to acknowledge project funding under the European Union's Seventh Framework Programme (FP7/2007-2013): grant n° 315313, BIOBOARD project (www.bioboard.eu). In addition, the authors would like to thank their respective colleagues N. Rodler and D. Schlemmer for fruitful discussions and support. Thanks are also extended to M. Pummer, T. Brandner, and M. Stenger for their assistance with material processing and process optimization.

REFERENCES

1. Jones, O. G.; McClements, D. *J. Compreh. Rev. Food Sci. Food Safety* **2010**, *9*, 374.
2. Reddy, N.; Yang, Y. *J. Appl. Polym. Sci.* **2013**, *130*, 729.
3. Park, J. W.; Scott Whiteside, W.; Cho, S. Y. *LWT-Food Sci. Technol.* **2008**, *41*, 692.
4. Verbeek, C. J. R.; van den Berg, L. E. *Macromol. Mater. Eng.* **2010**, *295*, 10.
5. Herrmann, P. S. D.; Yoshida, C. M. P.; Antunes, A. J.; Marcondes, J. A. *Pack. Technol. Sci.* **2004**, *17*, 267.
6. De Wit, J. N. Lehrbuch der Molke und Molkenerzeugnisse; European Whey Products Association: Brüssel, **2001**.
7. Fang, Y.; Tung, M. A.; Britt, I. J.; Yada, S.; Dalgleish, D. G. *J. Food Sci.* **2002**, *67*, 188.
8. Hong, S. I.; Krochta, J. M. *J. Food Sci.* **2003**, *68*, 224.
9. Hong, S.-I.; Krochta, J. M. *Pack. Technol. Sci.* **2004**, *17*, 13.
10. Kokoszka, S.; Debeaufort, F.; Lenart, A.; Voilley, A. *Int. Dairy J.* **2010**, *20*, 53.
11. McHugh, T.; Krochta, J. *J. Am. Oil Chem. Soc.* **1994**, *71*, 307.
12. McHugh, T. H.; Aujard, J. F.; Krochta, J. M. *J. Food Sci.* **1994**, *59*, 416.
13. Kurek, M.; Galus, S.; Debeaufort, F. *Food Pack. Shelf Life* **2014**, *1*, 56.
14. Schmid, M. Whey protein-based coatings as sustainable barrier material in food packaging applications IAPRI World Packaging Conference 2012, 2012 San Luis Obispo, California, USA. Lancaster, PA, USA: DEStech Publications, Inc., **2012**, 279–286.
15. Schmid, M.; Dallmann K.; Bugnicourt, E.; Cordoni, D.; Wild, F.; Lazzeri, A.; Noller, K. *Int. J. Polym. Sci.* **2012**, *7*, **2012**.
16. Bugnicourt, E.; Schmid, M.; Nerney, O. M.; Wildner, J.; Smykala, L.; Lazzeri, A.; Cinelli, P. *Adv. Mater. Sci. Eng.* **2013**, *2013*, 10.
17. Schmid, M.; Hinz, L.-V.; Wild, F.; Noller, K. *Materials* **2013**, *6*, 927.
18. Schmid, M.; Noller, K.; Wild, F.; Bugnicourt, E. WO Patent 2,013,014,493, **2013**.

19. Schmid, M. *Materials* **2013**, *6*, 3254.
20. Schmid, M.; Sängerlaub, S.; Wege, L.; Stäbler, A. Properties of Transglutaminase Crosslinked Whey Protein Isolate Coatings and Cast Films. *Pack. Technol. Sci.* **2014**, doi: 10.1002/pts.2071.
21. Schmid, M.; Hammann, F.; Winkler, H. Technofunctional Properties of Films Made From Ethylene Vinyl Acetate/Whey Protein Isolate Compounds. *Pack. Technol. Sci.* **2013**, *27*, 521.
22. Singh, P.; Saengerlaub, S.; Wani, A. A.; Langowski, H. C. *Pigment Resin Technol.* **2012**, *41*, 368.
23. Hernandez-Izquierdo, V. M.; Krochta, J. M. *J. Food Sci.* **2008**, *73*, R30.
24. Hernandez-Izquierdo, V. M. University of California, Davis: **2007**.
25. Barone, J. R.; Schmidt, W. F.; Gregoire, N. T. *J. Appl. Polym. Sci.* **2006**, *100*, 1432.
26. Plackett, D., Biopolymers: New Materials for Sustainable Films and Coatings; Wiley: Chichester, UK, **2011**.
27. Gupta, P.; Nayak, K. K. Characteristics of protein-based biopolymer and its application. *Polym. Eng. Sci.* **2014**, doi: 10.1002/pen.23928.
28. Abolhasani, M. M.; Azar, A. A.; Shokoohi, S. *J. Appl. Polym. Sci.* **2009**, *112*, 1716.
29. Gupta, A. K.; Ratnam, B. K.; Srinivasan, K. R. *J. Appl. Polym. Sci.* **1992**, *46*, 281.
30. John, B.; Varughese, K. T.; Oommen, Z.; Pötschke, P.; Thomas, S. *J. Appl. Polym. Sci.* **2003**, *87*, 2083.
31. Mészáros, L.; Fejős, M.; Bárány, T. *J. Appl. Polym. Sci.* **2012**, *125*, 512.
32. Takidis, G.; Bikiaris, D. N.; Papageorgiou, G. Z.; Achilias, D. S.; Sideridou, I. *J. Appl. Polym. Sci.* **2003**, *90*, 841.
33. Bhattacharyya, A. R.; Maiti, S. N.; Misra, A. *J. Appl. Polym. Sci.* **2002**, *85*, 1593.
34. Zhang, F.; Sundararaj, U. *Polym. Compos.* **2004**, *25*, 535.
35. Zou, H.; Ma, Q.; Tian, Y.; Wu, S.; Shen, J. *Polym. Compos.* **2006**, *27*, 529.
36. Anonymous. Product data sheet: EVA Evateno HM 150, Braskem, Frankfurt am Main, Germany, Ed.: 2007.
37. Brockes, A.; Berger-Schunn, A.; Strocka, D. Farbmessung in der Textilindustrie; Farbenfabriken Bayer AG: Leverkusen, **1986**.
38. Peeterbroeck, S.; Laoutid, F.; Taulemesse, J. M.; Monteverde, F.; Lopez-Cuesta, J. M.; Nagy, J. B.; Alexandre, M.; Dubois, P. *Adv. Funct. Mater.* **2007**, *17*, 2787.
39. Shen, C. H.; Wang, Y. Y. *Die Angewandte Makromolekulare Chemie* **1984**, *121*, 49.
40. Verbeek, C. J. R.; Van Den Berg, L. E. *Macromol. Mater. Eng.* **2010**, *295*, 10.
41. Sothornvit, R.; Reid, D. S.; Krochta, J. M. *Transact. Asae* **2002**, *45*, 1479.
42. Anker, M.; Stading, M.; Hermansson, A. M. *J. Agr. Food. Chem.* **1999**, *47*, 1878.
43. Zhang, J.; Mungara, P.; Jane, J. *Polymer* **2001**, *42*, 2569.
44. Frick, A.; Stern, C. DSC- Prüfung in der Anwendung; Hanser: München, **2006**.
45. Thomas, S.; Groeninckx, G. *J. Appl. Polym. Sci.* **1999**, *71*, 1405.
46. Peanasky, J. S.; Long, J. M.; Wool, R. P. *J. Polym. Sci. Part B: Polym. Phys.* **1991**, *29*, 565.
47. Wu, P. C.; Jones, G.; Shelley, C.; Woelfli, B. *J. Eng. Fiber Fabr.* **2007**, *2*, 49.
48. Giancola, G.; Lehman, R. L.; Miller, S. *Polym. Eng. Sci.* **2012**, *52*, 1548.
49. Potschke, P.; Paul, D. R. *J. Macromol. Sci-Pol. R* **2003**, *C43*, 87.
50. Sothornvit, R.; Olsen, C. W.; McHugh, T. H.; Krochta, J. M. *J. Food Sci.* **2003**, *68*, 1985.
51. Endres, H.-J. S.-R. In Technische Biopolymere – *Rahmenbedingungen, Marktsitutation, Herstellung, Aufbau und Eigenschaften;* Hanser Fachbuchverlag, München, **2009**. ISBN: 9783446416833.
52. Khwaldia, K.; Arab-Tehrany, E.; Desobry, S. *Compreh. Rev. Food Sci. Food Safety* **2010**, *9*, 82.